Elsevier Editorial System(tm) for International Journal of Radiation Oncology*Biology*Physics
Manuscript Draft

Manuscript Number:

Title: Development of a MicroCT-Based Image-Guided Conformal Radiotherapy System for Small Animals

Article Type: Full Length Article

Section/Category: Physics Contribution

Keywords: Mouse models; Radiotherapy; Image guidance; MicroCT

Corresponding Author: Dr. Edward Graves, PhD

Corresponding Author's Institution: Stanford University

First Author: Hu Zhou, PhD

Order of Authors: Hu Zhou, PhD; Manuel Rodriguez, PhD; Fred van den Haak; Geoffrey Nelson; Rahil Jogani; Jiali Xu; Xinzhi Zhu, PhD; Yongjiang Xian; Phuoc T Tran, MD; Dean W Felsher, MD, PhD; Paul J Keall, PhD; Edward Graves, PhD

Abstract: Purpose
The need for clinically-relevant radiation therapy technology for the treatment of preclinical models of disease has spurred the development of a variety of dedicated platforms for small animal irradiation. Our group has taken the approach of adding the ability to deliver conformal radiotherapy to an existing 120 kVp micro-computed tomography (microCT) scanner.
Methods
A GE eXplore RS120 microCT scanner was modified by the addition of a two-dimensional subject translation stage and a variable aperture collimator. Quality assurance protocols for these devices, including measurement of translation stage positioning accuracy, collimator aperture accuracy, and

collimator alignment with the x-ray beam, were devised. Use of this system for image-guided radiotherapy was assessed by irradiation of a solid water phantom as well as of two mice bearing spontaneous MYC-induced lung tumors. Radiation damage was assessed ex vivo by immunohistochemical detection of γH2AX foci.

Results

The positioning error of the translation stage was found to be less than 0.05 mm, while after alignment of the collimator with the x-ray axis through adjustment of its displacement and rotation, the collimator aperture error was less than 0.1 mm measured at isocenter. CT image-guided treatment of a solid water phantom demonstrated target localization accuracy to within 0.1 mm. γH2AX foci were detected within irradiated lung tumors in mice, with contralateral lung tissue displaying background staining.

Conclusions

Addition of radiotherapy functionality to a microCT scanner is an effective means of introducing image-guided radiation treatments into the preclinical setting. This approach yields high radiotherapy performance while leveraging existing technology.

Suggested Reviewers: David Jaffray
Princess Margaret Hospital
david.jaffray@rmp.uhn.on.ca
Dr. Jaffray is also developing small animal radiotherapy technology.

Eric Ford
Johns Hopkins University
EFord6@jhmi.edu
Dr. Ford is also developing small animal radiotherapy technology.

Daniel Low
Washington University
dlow@radonc.wustl.edu
Dr. Low is also developing small animal radiotherapy technology.

Eugene Wong
University of Western Ontario
ewong4@uwo.ca

Dr. Wong has worked with the GE microCT and investigated it as a vehicle for small animal radiotherapy.

Opposed Reviewers:

* Cover Letter

April 18, 2009

James D. Cox, Editor-in-Chief
International Journal of Radiation Oncology Biology Physics
Editorial Office
Scientific Publications-227
The University of Texas M.D. Anderson Cancer Center
1515 Holcombe Blvd.
Houston, TX 77030

Dear Dr. Cox:

I have enclosed the text, figures, and tables of a manuscript entitled ***"Development of a MicroCT-Based Image-Guided Conformal Radiotherapy System for Small Animals"*** for consideration for publication in the *International Journal of Radiation Oncology Biology Physics*. This paper reports on the engineering of a system for the treatment of small animals with clinically-relevant image-guided radiotherapy. The system is based on a microCT scanner, giving it both established imaging capabilities as well as allowing for rapid commercialization of the device. The manuscript reports on the design and construction of this system, as well as evaluation of its IGRT performance in both phantoms and *in vivo* in spontaneous murine tumors. The work described by our group presents a strategy for incorporating clinical radiotherapy capabilities in preclinical studies that is an alternative to those discussed by Wong et al. (Volume 71, No. 5, 1591-1599) and Cai et al. (Volume 73, No. 5, 1588-1595) in recent issues of your journal. We feel that this paper describes a practical method for bringing conformal radiotherapy to the laboratory, and is of keen interest to readers of the *International Journal of Radiation Oncology Biology Physics* as this exciting topic comes to fruition. We hope that you will share our enthusiasm, and look forward to hearing your comments on the manuscript.

Sincerely,

Edward Graves, Ph.D.
Assistant Professor
Department of Radiation Oncology
Stanford University
875 Blake Wilbur Dr., CC-G202
Stanford, CA 94305-5847

phone: (650) 723-5591
fax: (650) 498-4015
email: egraves@stanford.edu

Development of a MicroCT-Based Image-Guided Conformal Radiotherapy System for Small Animals

Hu Zhou[1], Ph.D., Manuel Rodriguez[1], Ph.D., Fred van den Haak[1], Geoffrey Nelson[1], Rahil Jogani[1], Jiali Xu[3], Xinzhi Zhu[3], Ph.D., Yongjiang Xian[4], Phuoc T. Tran[1], M.D., Dean W. Felsher[2], M.D., Ph.D., Paul J. Keall[1], Ph.D., Edward E. Graves[1], Ph.D.

Departments of Radiation Oncology[1] and Medicine[2]
Molecular Imaging Program at Stanford
Stanford University
Stanford, CA 94305 USA

PheniCo Inc.[3]
Fremont, CA 94538

Bright Star Machine[4]
Fremont, CA 94538

*Address correspondence to: Edward E. Graves, Ph.D.
Department of Radiation Oncology
Stanford University
875 Blake Wilbur Dr., Room G-202
Stanford, CA 94305-5847

phone: (650) 723-5591
fax: (650) 498-4015
email: egraves@stanford.edu

Running title: Small Animal Image-Guided Radiotherapy

Conflict of Interest

The authors certify that no conflicts of interest related to the contents of this report exist.

Abstract

Purpose

The need for clinically-relevant radiation therapy technology for the treatment of preclinical models of disease has spurred the development of a variety of dedicated platforms for small animal irradiation. Our group has taken the approach of adding the ability to deliver conformal radiotherapy to an existing 120 kVp micro-computed tomography (microCT) scanner.

Methods

A GE eXplore RS120 microCT scanner was modified by the addition of a two-dimensional subject translation stage and a variable aperture collimator. Quality assurance protocols for these devices, including measurement of translation stage positioning accuracy, collimator aperture accuracy, and collimator alignment with the x-ray beam, were devised. Use of this system for image-guided radiotherapy was assessed by irradiation of a solid water phantom as well as of two mice bearing spontaneous MYC-induced lung tumors. Radiation damage was assessed *ex vivo* by immunohistochemical detection of γH2AX foci.

Results

The positioning error of the translation stage was found to be less than 0.05 mm, while after alignment of the collimator with the x-ray axis through adjustment of its displacement and rotation, the collimator aperture error was less than 0.1 mm measured at isocenter. CT image-guided treatment of a solid water phantom demonstrated target localization accuracy to within 0.1 mm. γH2AX foci were detected within irradiated lung tumors in mice, with contralateral lung tissue displaying background staining.

Conclusions

Addition of radiotherapy functionality to a microCT scanner is an effective means of introducing image-guided radiation treatments into the preclinical setting. This approach yields high radiotherapy performance while leveraging existing technology.

Keywords: Mouse models, Radiotherapy, Image guidance, MicroCT

A. Introduction

Clinical radiation therapy (RT) technology has advanced tremendously since the introduction of the linear accelerator in 1956. Advances such as rotating radiation sources, conformal collimators, inverse treatment planning, image guidance and verification, and motion management are now commonplace among modern RT equipment. However, analogous systems for the treatment of laboratory animals lack many of these now standard clinical features. Delivery of radiation treatments to experimental animal models of disease has typically been achieved using fixed radiation sources applying a single radiation field. Sparing of normal tissues using this approach is limited to use of radiation shields, commonly sheets of lead of custom-manufactured jigs, bearing openings through which the desired radiation target within the animal is exposed (1-5). The spatial and dosimetric accuracies achievable with these systems are clearly limited, and lag significantly behind their clinical counterparts. Except in the case of superficial targets, precise localization of the radiation target as well as sparing of normal tissues are usually not possible with this simple approach.

Recently several 3D conformal animal RT systems have been developed in an effort to bridge the gap between preclinical and clinical radiotherapy technology. Stojadinovic and colleagues have constructed a radiotherapy system around a clinical ^{192}Ir high dose rate brachytherapy source, delivering beams restricted by fixed collimators from multiple angles to irradiate animals similar to conformal radiotherapy (6). Other groups have built systems from scratch utilizing x-ray tubes for application of diagnostic (imaging) and therapeutic (treatment) radiation. Lindsay *et al*. have mounted a 225 kVp x-ray tube on a C-arm gantry within a shielded hot cell for treatment of animals (7). Wong and colleagues have built a standalone system encompassing a 225 kVp industrial x-ray tube and individually rotating x-ray, detector, and subject enclosures

that can be used to deliver noncoplanar radiation beams to animals (8). Our group has addressed this technical challenge by adding radiotherapy functionality to a microCT scanner in an attempt to leverage existing technology to produce a preclinical system for image-guided radiation therapy (IGRT) (9). In this article we report on the physical aspects of this system as well as evaluation of the accuracy of this instrument. In addition, we demonstrate the application of this technology for irradiating tumors growing within the lungs of mice.

B. Methods and Materials

B.1. System

B.1.1. *GE RS120 MicroCT*

An eXplore RS120 microCT scanner (GE Medical Systems, London, Ontario, Canada) served as the platform for the development of a radiation delivery system. **Figure 1a** shows the scanner gantry. The body of the scanner, including the gantry on which the imaging system components are mounted and a cable rack through which the control PC communicates with these components, are enclosed in a lead shield. The CT isocenter is located at the center of a plexiglass tube (the CT bore). The x-ray tube and detector are fixed on the gantry on opposite sides of the bore. The RS120 microCT system has a stage housing inside which an animal couch stage moves along the CT axial direction (the z-axis in the CT coordinate system) to carry the animal into and out from the bore for imaging. A nose cone on this bed allows the continuous delivery of isoflurane anesthesia to a subject while it is on the scanner bed. The housing provides an x-ray shield separate from the scanner itself to prevent radiation from exiting the device.

In order to serve as a radiotherapy device, this system requires several additional functionalities that are not necessary for microCT imaging. These added capabilities include the ability to restrict the width of the beam to target a specific volume of tissue, and the ability to shift an arbitrary three-dimensional point within a subject to the system isocenter for treatment. To meet these needs, we integrated a two-dimensional translation stage with the existing z-stage inside the shield to accomplish 3D movement, and mounted a variable-aperture collimator between the source and the bore on the crossbar shown in **Figure 1d**.

B.1.2. *Animal Couch*

The microCT includes an animal couch clamped on a motor-driven stage that moves the animal in and out of the scanner along the z-direction, installed inside the x-ray shielded stage housing. We incorporated a 2D stage that moves in the two other directions (x or left/right, and y or up/down) inside the housing, as shown in **Figure 1b**. To move the stage within the 10.2 cm bore, the maximum travel distance in x and y were designed to be 50.8 mm and 20 mm, respectively. The 2D stage is installed on the existing z-stage mount by opening and closing a clamp, and can be moved either manually through a control box or through software controls installed on the microCT control PC.

B.1.3. *Collimator*

A variable-aperture collimator installed on the scanner gantry between the x-ray source and the subject bore allows the shaping of the x-ray beam for radiotherapy, or alternately passage of the full beam for imaging. The design goal of the collimator was to vary the x-ray beam diameter from 0 (fully closed) to 102 mm (fully open) at the CT isocenter. The attenuation in the shielded area was designed to be more than 95%. The complete collimator assembly and its placement on the scanner gantry is shown in **Figure 1d**.

Figure 1c shows the principle of the collimator, in which 12 pentagonal lead-brass blocks were arranged in two planes, forming two stages of collimation. The simultaneous sliding of the 6 blocks of each stage along their respective linear tracks forms a regular hexagonal aperture, whose width can be adjusted by the positions of the blocks. The two hexagonal apertures are arranged coaxially, offset by 30°, and each is driven by a stepper motor through a lead screw. The two stages will hereafter be referred to as the "near" collimator (closest to the x-ray source) and the "far" collimator. By setting the size of the two apertures to a constant ratio, equal to the distance ratio of the two hexagons from the x-ray source spot, a regular dodecagon beam profile is formed. This design improves upon a previous rotationally-driven implementation (9) by moving to a more robust linear driving scheme. A position sensor attached to each stage reports the aperture size of the stage. A brass plate with a circular opening, attached to near side of the collimator, shields the control electronics within the device from irradiation. A graphical user interface (GUI) on the microCT control PC allows the user to specify collimator apertures, either independently or synchronized in order to fit the divergence of the x-ray beam.

B.1.4. *Treatment Planning System*

A treatment planning system is under development. This system includes a GUI based on the RT_Image software package (10) and is linked to a Monte Carlo dose computation system based on the EGSnrc code. The GUI allows the user to manually specify a sequence of beams, setting the isocenters, widths, angular directions, and exposure times for each. Work is ongoing to incorporate inverse planning techniques into this application, and to design a custom device control application that can deliver a treatment plan created in RT_Image.

B.2. Calibration

B.2.1. *Translation stage*

The geometric calibration of the translation stage determined the relationship between the physical positions and the machine units of the stages. In the calibration each stage was set with a series of machine units and the physical positions were measured after each movement. The stages were repeatedly moved back and forth to determine the effects of any potential mechanical backlash.

B.2.2. *Collimator*

B.2.2.1. *Geometric calibration*

The geometric calibration of the collimator included two major measurements: the physical aperture versus machine unit calibration, and the collimator-beam axis alignment. The physical aperture/machine control unit calibration was performed to determine the relationship between the physical aperture size and the machine readings. To find the parameters of this relationship, several cylinders with diameters ranging from 6 mm to 36 mm with precisions of 0.025 mm were prepared. For each measurement, one of these cylinders was inserted in the aperture of one fully open collimator stage, and the aperture was then reduced until the cylinder was tightly held. The position sensor reading at this location was recorded. These readings were then fit to a linear function of the cylinder diameter to obtain the calibration parameters. The measurement was repeated several times with the aperture setting from nearly closed to fully open, and from fully open to nearly closed, to measure the uncertainty of the movement and possible backlash.

B.2.2.2. *Alignment with x-ray beam*

The x-ray beam axis is defined as a straight line passing the source spot center and perpendicular to the CT axis. Alignment of the collimator axis with this line was necessary to ensure that the collimator focuses the radiation beam on the isocenter regardless of aperture size. A misalignment can be decomposed to displacement and tilting: the collimator axis may be displaced from the beam axis, and the collimator axis may be tilted with respect to the beam axis. Displacement was measured through several methods, including a split field test (11), imaging of a fixed object through a collimator at angles of 0° and 180°, and by evaluation of the hexagonal profiles produced by each of the two collimator stages (9). A small tilt of the collimator plane creates an effect similar to displacement in the appearance of the hexagonal profiles of the collimator stages. If the displacement is assumed to be zero, the angle of tilting can be derived from the law of sines. The composite alignment procedure therefore consisted of iterative measurement and correction of the displacement and tilting of the collimator until the error fell within a tolerance of 0.1 mm. Several sets of positioning screws were set to allow reproducible translation and angular positioning of the collimator.

B.2.2.3. *Collimator performance*

When adjusting the collimator aperture, the control software compares the current sensor reading with the user-specified new aperture size to calculate the required shift. After performing this shift, the software makes this comparison again and iterates this process until the discrepancy between the desired and actual aperture sizes is below a tolerance. The error tolerance of the collimator aperture measured at the CT isocenter was set to 0.1 mm when the aperture is larger than 20 mm, and 0.05 mm for smaller apertures. These error tolerances were chosen in an effort to balance device accuracy with collimator adjustment time. The performance of the collimator was measured by repeatedly setting the collimator with different apertures and recording the

aperture size error and the setting time, to evaluate the reliability of the mechanism and the control algorithm.

B.3. Phantom irradiation

In order to establish that this hybrid microCT/RT system could accurately localize an arbitrary target within a subject for irradiation, a phantom was constructed. The phantom consisted of ten sheets of solid water measuring 3 x 3 x 0.3 cm stacked to form a cube. Within one of the central sheets, a hole of diameter 0.3 cm was drilled at a location of (10 mm, 10 mm) from the upper left corner. A 3 mm diameter metal sphere was secured in the center of this hole, and sheets of radiochromic film were sandwiched within the solid water stack above and below the sheet bearing the sphere. This phantom was then placed on the microCT subject bed and secured so that the films and solid water sheets were coplanar with the plane of rotation of the scanner gantry. The phantom was imaged using a standard microCT protocol (400 views, 0.9° view increment, 70 kV, 40 mA, 25 ms exposure per view). The image data was reconstructed at an isotropic resolution of 0.1 mm per pixel and viewed with RT_Image. The location of the metal sphere was identified in the microCT images, and the translation stage offsets needed to shift the sphere to the scanner isocenter were calculated. These offsets were applied, and subsequently the phantom was irradiated with 8 beams spaced at 45° increments, using exposure times calculated from beam commissioning data to deliver a total dose of 1 Gy at isocenter (12). The film was then removed and the dose profile on it was used to assess the accuracy of targeting of the metal sphere.

B.4. Mouse irradiation

To assess whether this unit could be used to deliver conformal radiotherapy to a murine subject, we irradiated tumors in the lungs of two mice to a dose of 2 Gy at isocenter. Transgenic mice were created that, when treated with tetracycline, specifically express the MYC oncogene in the cells of the lung. These mice develop spontaneous lung carcinomas within a median of 52 weeks of MYC induction (13). Two of these mice bearing late-stage disease (greater than 52 weeks post-induction) were selected for treatment with radiotherapy. A subject mouse was placed on the microCT bed and anesthetized with isoflurane, delivered continuously through a nose cone on the bed. MicroCT data was acquired as 400 projections equally spaced over 360° (tube voltage 70 kV, tube current 40 mA, 25 ms exposure per projection), which were then reconstructed into volumetric CT images using a cone beam algorithm. The reconstructed 3D volume was loaded into RT_Image to localize the desired target and calculate the appropriate position settings for the 3D translation stage and the collimator. After adjusting the stages and collimator, radiotherapy was delivered as a series of 8 beams equally spaced over 360° to a dose of 2 Gy at isocenter. A Monte Carlo model was used to simulate the dose distribution produced by this treatment (14).

Immediately following irradiation, the mice were sacrificed and tissues were harvested. The lungs of the mice, including the target tumors, were excised, fixed in formalin, and cut into 20 mm sections. They were then stained with antibodies against γH2AX, a histone protein that is recruited to the site of double strand breaks (15), as well as DAPI to visualize cell nuclei. These immunohistochemical sections were then visualized with fluorescence microscopy. As the mice developed multiple lesions within the lungs, comparisons were made in γH2AX staining between

the tumor on which radiation was focused and other tumors that received background levels of radiation.

C. Results

C.1. System

C.1.1. *Collimator*

The custom-designed collimator was installed on the microCT gantry successfully. The weight of the collimator assembly was 17 pounds, which was counterweighted on the gantry by the addition of lead disk weights to the outer cylindrical counterweights. MicroCT images acquired before and after installation of the collimator demonstrated no measurable degradation in image quality following addition of the collimator.

C.2. Calibration

C.2.1. *Translation stage*

The motors driving the translation stage in x and y have resolutions of 787.6 and 1400.9 steps/mm, respectively. The reproducibility, determined by comparing the physical position of the device and the motor readings, is better than 0.05 mm in both directions.

C.2.2. *Collimator*

C.2.2.1. *Geometric calibration*

The machine unit/physical aperture relationship was measured by inserting the cylinders of different standard diameters and reading the position sensors of the collimator, from which linear relations were obtained for the near and far stages. The fitting uncertainty was 0.15% on average (maximum 0.36%), obtained from the variation of repeated measurements. The size of these apertures at the isocenter was then measured using both radiochromic film and the CT detector,

allowing expression of the relationship between the collimator machine units and the aperture sizes. These relationships were implemented in the collimator control software.

C.2.2.2. *Alignment with x-ray beam*

The collimator alignment procedure required 5 iterations of the displacement-tilting adjustment and measurement. **Figure 2** demonstrates the split field, imaged object, and two hexagon measurement techniques used to assess displacement. In addition to the displacements required to align the collimator with the beam, a slight tilt was noted that was corrected by elevating the left side of the collimator by 1.4 mm. The displacement and tilting adjustments measured after completion of the alignment procedure were less than 0.1 mm.

C.2.2.3. *Collimator performance*

The results of the performance measurements are listed in **Table 1**. Aperture sizes at isocenter could be achieved by the control software with errors of less than 1.0%. Adjustment of the collimator from a fully open position to an aperture relevant for small animal radiotherapy required between 20 and 40 seconds in order to iterate to the desired tolerable error.

C.3. Phantom irradiation

Figure 3 shows the results of a test designed to evaluate the ability of the system to locate and deliver radiation beams to a target within a subject. A metal sphere served as a CT-visible target within a cubic solid water phantom. Streak and ring artifacts are visible in the reconstructed CT image because of high x-ray attenuation within the sphere. The centroid of the received dose distribution colocalized with the position of the target metal sphere to within ±0.5 mm in the x and y scanner axes. Because of the two dimensional nature of film measurement and the fact

that two films sandwiching the sphere-bearing solid water sheet were used, the accuracy along the z axis can only be approximated to ±3 mm.

C.4. Mouse irradiation

Results obtained from irradiation of a tumor-bearing mouse are shown in **Figure 4**. Simulation of the dose distribution achieved by a simple 8 field plan using 8 mm beams reveals that the dose to the target achieved the desired level of 2 Gy, while doses to surrounding lung were in the range of 0.3 Gy. A star pattern is visible due to the small numbers of beams used. The total treatment time required for this plan, including setup and delivery, was 45 minutes. Sections collected from the target tumor immediately after irradiation showed the presence of γH2AX foci, indicating the formation of DNA double strand breaks. Sections taken from contralateral lung that received a low dose show only background staining.

D. Discussion

Micro-computed tomography presents an intriguing platform for the engineering of small animal radiotherapy devices because of the advanced state of development of this technology as well as the suitability of kilovoltage x-ray beams for treating small subjects. We have pursued this possibility by adding hardware and software to an existing scanner in order to produce a hybrid imaging and radiotherapy system. The two-dimensional translation stage and variable aperture collimator needed to introduce radiotherapy capability to this system can be manufactured at a cost of less than $25,000, facilitating commercial development of this system as a low-cost add-on option to existing microCT scanners. The utility of this system was demonstrated through irradiation of both a phantom as well as a tumor-bearing mouse. Experiments using a phantom demonstrated that the combination of the translation stage, collimator, and microCT apparatus

can provide submillimeter targeting accuracy. This capability was applied *in vivo* by delivering a radiation treatment to a transgenic mouse bearing a spontaneous MYC-induced lung tumor. The results of this experiment demonstrate the potential for treatment of sophisticated orthotopic and spontaneous models of disease using this preclinical image-guided radiotherapy approach.

Based on the Monte Carlo dosimetry simulation generated for the lung tumor irradiation, it is apparent that the kilovoltage beams of this system deliver significant doses to bony structures. At present it is unknown whether this dose will limit the application of this system. It is well known that the mass attenuation coefficient of human bone is approximately an order of magnitude greater at the kilovoltage energies of this system relative to the megavoltage energies of clinical radiotherapy systems, however the elemental composition and density of mouse bone have not been rigorously studied. Recent Monte Carlo material modeling efforts have suggested that more rigorous treatment of bony tissues in Monte Carlo simulations is required in this context, and suggests that the dose to mouse bones may be overestimated when using material properties derived from human bones (14). Ultimately the problem of bone dose in radiotherapy is not unique to this system, it is relevant to the vast majority of single field and conformal systems reported to date that employ kilovoltage x-ray beams.

The increase in temperature in the x-ray generator and its thermal limits provide constraints on the length of radiotherapy treatments and correspondingly the doses that can be delivered. Because the x-ray tube operates in a pulsed fashion, we found that using a longer pulse interval (reduced duty cycle) together with periodic short (1-3 minute) breaks can significantly reduce generator heating. Improving heat dissipation within the generator or replacing the generator with a more powerful model will reduce this limitation. However, heating of the x-ray tube is a second important consideration. Replacement of the x-ray tube with a more robust model, or

alternately use of a larger focal spot at the cost of increased beam penumbra, may be required for extended radiotherapy protocols.

This work has shown that it is technically possible to modify a microCT scanner to serve as a small animal conformal radiotherapy system, operating in a fashion analogous to current clinical image-guided radiotherapy devices. We anticipate that the applications of radiation in molecular biology studies of animal tumors using technology such as that demonstrated here will significantly enhance our knowledge of radiobiology and provide a means to study clinically-relevant radiation treatment strategies in a preclinical setting.

E. References

1. Knox SJ, Goris ML, Wessels BW. Overview of animal studies comparing radioimmunotherapy with dose equivalent external beam irradiation. *Radiotherapy and Oncology* 1992;23:111-117.

2. Khan MA, Hill RP, Van Dyk J. Partial volume rat lung irradiation: an evaluation of early DNA damage. *International Journal of Radiation Oncology Biology Physics* 1998;40:467-476.

3. Hillman GG, Maughan RL, Grignon DJ*, et al.* Neutron or Photon Irradiation for Prostate Tumors: Enhancement of Cytokine Therapy in a Metastatic Tumor Model. *Clinical Cancer Research* 2001;7:136-144.

4. Khan MA, Van Dyk J, Yeung IW*, et al.* Partial volume rat lung irradiation: assessment of early DNA damage in different lung regions and effect of radical scavengers. *Radiotherapy and Oncology* 2003;66:95-102.

5. Hillman GG, Wang Y, Che M*, et al.* Progression of renal cell carcinoma is inhibited by genistein and radiation in an orthotopic model. *BMC Cancer* 2007;7:4.

6. Stojadinovic S, Low D, Hope A*, et al.* MicroRT—Small animal conformal irradiator. *Medical Physics* 2007;34:4706.

7. Lindsay P, Ansell S, Moseley D*, et al.* Development of An Image-Guided Conformal Small Animal Irradiation Platform. Annual Meeting of the American Association of Physicists in Medicine. Houston, TX; 2008. p. 2695.

8. Wong J, Armour E, Kazanzides P*, et al.* High-Resolution, Small Animal Radiation Research Platform With X-Ray Tomographic Guidance Capabilities. *International Journal of Radiation Oncology Biology Physics* 2008;71:1591-1599.

9. Graves E, Zhou H, Chatterjee R*, et al.* Design and evaluation of a variable aperture collimator for conformal radiotherapy of small animals using a microCT scanner. *Medical Physics* 2007;34:4359-4367.

10. Graves EE, Quon A, Loo BW. RT_Image: An Open-Source Tool for Investigating PET in Radiation Oncology. *Technology in Cancer Research and Treatment* 2007;6:111-121.

11. Lutz WR, Larsen RD, Bjärngard BE. Beam alignment tests for therapy accelerators. *International Journal of Radiation Oncology Biology Physics* 1981;7:1727-1731.

12. Rodriguez M, Zhou H, Graves E*, et al.* Dosimetry of a Novel MicroCT/RT System for Small Animal Conformal Radiotherapy. Annual Conference of the American Association of Physicists in Medicine. Houston, TX; 2008.

13. Tran PT, Fan AC, Bendapudi P*, et al.* Combined Inactivation of MYC and K-Ras Oncogenes Reverses Tumorigenesis in Lung Adenocarcinomas and Lymphomas. *PLoS ONE* 2008;3:e2125.

14. Zhou H, Keall PJ, Graves EE. A Bone Composition Model for Monte Carlo X-Ray Transport Simulations. *Medical Physics* 2009;36:1008-1018.

15. Rogakou EP, Pilch DR, Orr AH*, et al.* DNA Double-stranded Breaks Induce Histone H2AX Phosphorylation on Serine 139. *Journal of Biological Chemistry* 1998;273:5858-5868.

345

F. Figure Legends

Figure 1. The GE RS120 microCT and the additional components necessary for small animal radiotherapy. A: A view of the scanner gantry after removing the x-ray shield and animal stage housing. The large silver disk is the rotating gantry, with the x-ray tube, H-shaped collimator mounting bar, subject bore, and detector arranged bottom to top, respectively. B: The custom two-dimensional translation stage for subject positioning, mounted on top of the existing z-axis translation stage of the scanner. C: Schematic representation of a single stage of the variable-aperture collimator, formed by six sliding blocks mounted on linear tracks. D: The final two-stage collimator apparatus after installation on the H mounting bar of the scanner gantry.

Figure 2. Measurement of collimator alignment with the x-ray beam axis. A: Split field irradiation. The offset o_x between the images from 0° (darker) and 180° (lighter) gantry angles is used to compute the offset of the collimator from the beam axis. B: Measurement of collimator offset by imaging a fixed object. The average of the object location seen at 0° and at 180° gives the scanner isocenter, while the collimator center can be measured based on the hexagonal profile. C: Measurement of collimator offset by fitting the hexagonal profiles produced by each collimator stage, with both stages set at isocenter apertures of 20 mm. Asymmetry in the dodecagon is apparent, produced by offset between the centers of the two hexagons. The white scale bar is of length 2.5 mm at isocenter. D: Two hexagon analysis following iterative alignment of the collimator with the x-ray beam axis. The collimator apertures are set to 10 mm at isocenter to improve visual detection of any misalignment. The white scale bar is of length 2.5 mm at isocenter.

Figure 3. Evaluation of subject targeting accuracy using a solid water phantom. A: A phantom containing a metal sphere and radiochromic film was placed on the scanner bed and imaged with microCT. B: The microCT image of the phantom showing the metal inclusion, and the radiation treatment plan that was constructed in RT_Image. C: The solid water sheet in which a hole was drilled and a metal sphere was placed. Sheets of radiochromic film were placed above and below this sheet. D: The radiochromic film after delivery of 8 x-ray beams to the target located by the metal sphere on the CT images. The center of the dose distribution measured on the film agreed with the location of the metal sphere to within 0.1 mm.

Figure 4. Treatment of a murine spontaneous lung tumor with the microCT radiotherapy system. A-C: A MYC-induced tumor growing in the base of the right lung of a mouse was imaged with microCT, shown in axial, coronal, and sagittal sections with the tumor volume outlined in red. D: A treatment consisting of 8 beams of diameter 8 mm at isocenter with angular spacing of 45º was constructed in RT_Image to irradiate the target (red) to a dose of 2 Gy. E: Monte Carlo simulation of the dose delivered by this plan, with the 1, 1.4, and 1.8 Gy isodose contours shown in green, yellow, and red, respectively. F: γH2AX (green) and DAPI immunohistochemical sections from the target tumor. G: Corresponding immunohistochemical sections from the left lung that received an average dose of 0.3 Gy.

Figure 1
Click here to download Figure: hz_figures_ijrobp 1.pdf

Figure 1

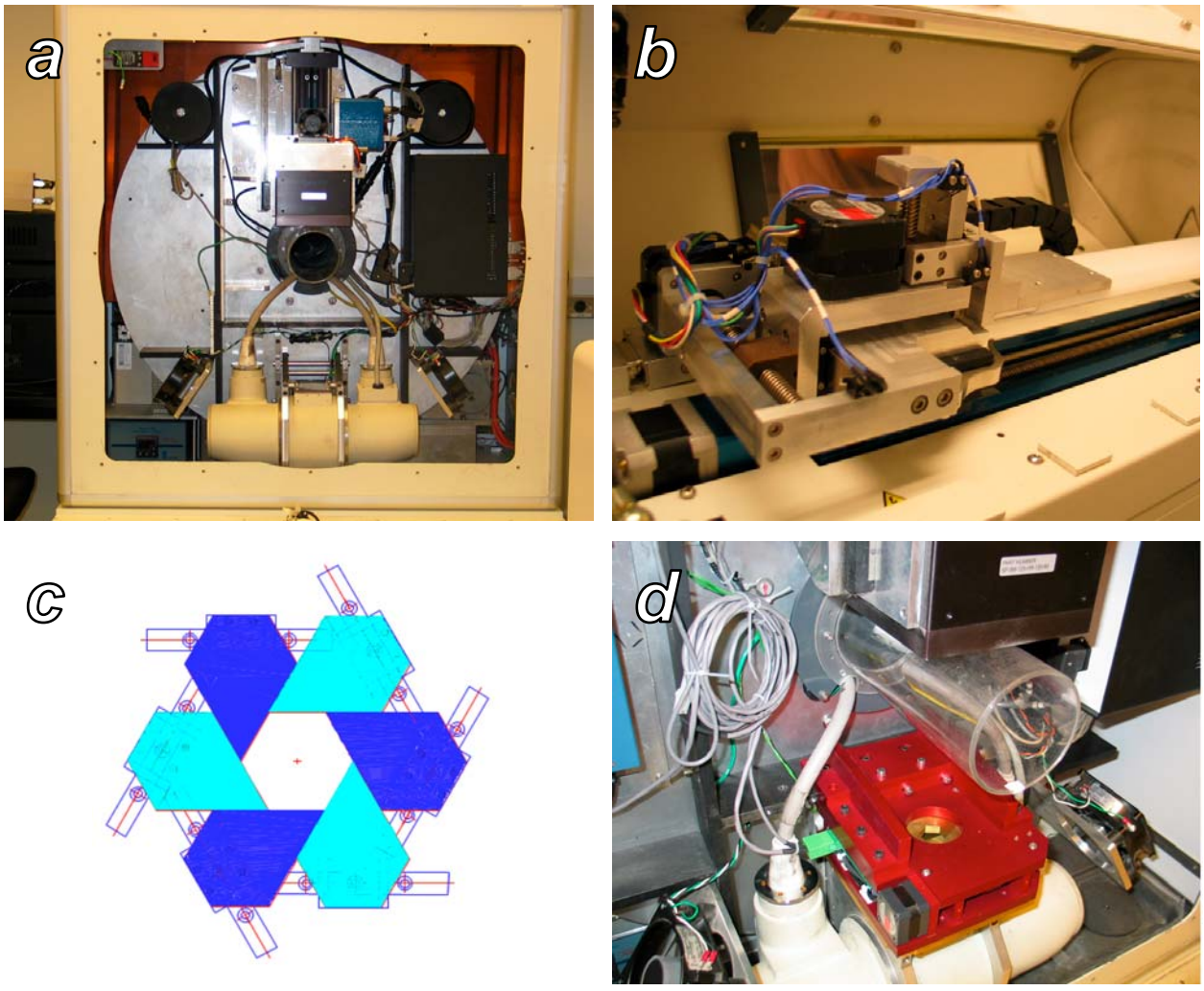

Figure 2
Click here to download Figure: hz_figures_ijrobp 2.pdf

Figure 2

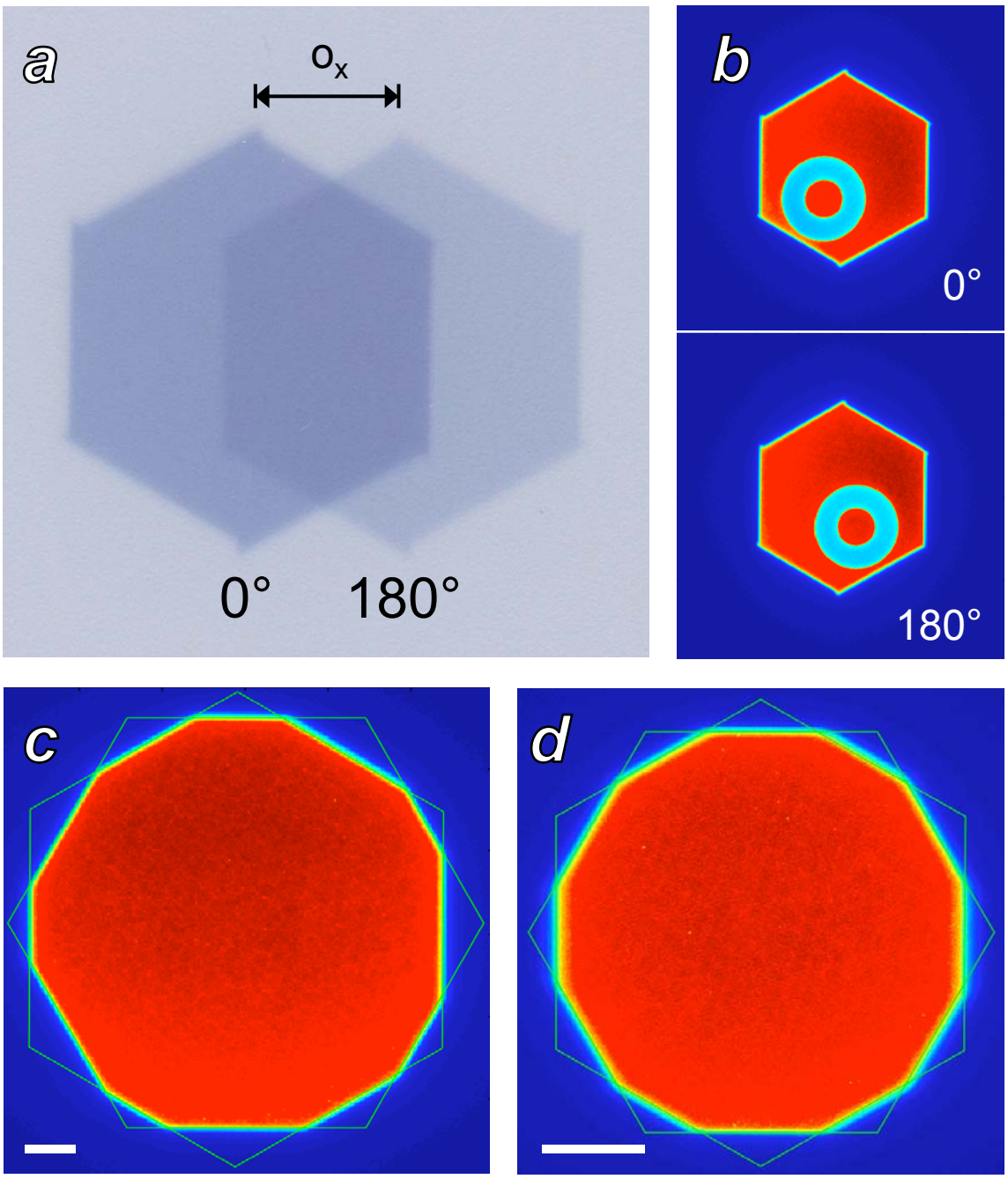

Figure 3
Click here to download Figure: hz_figures_ijrobp 3.pdf

Figure 3

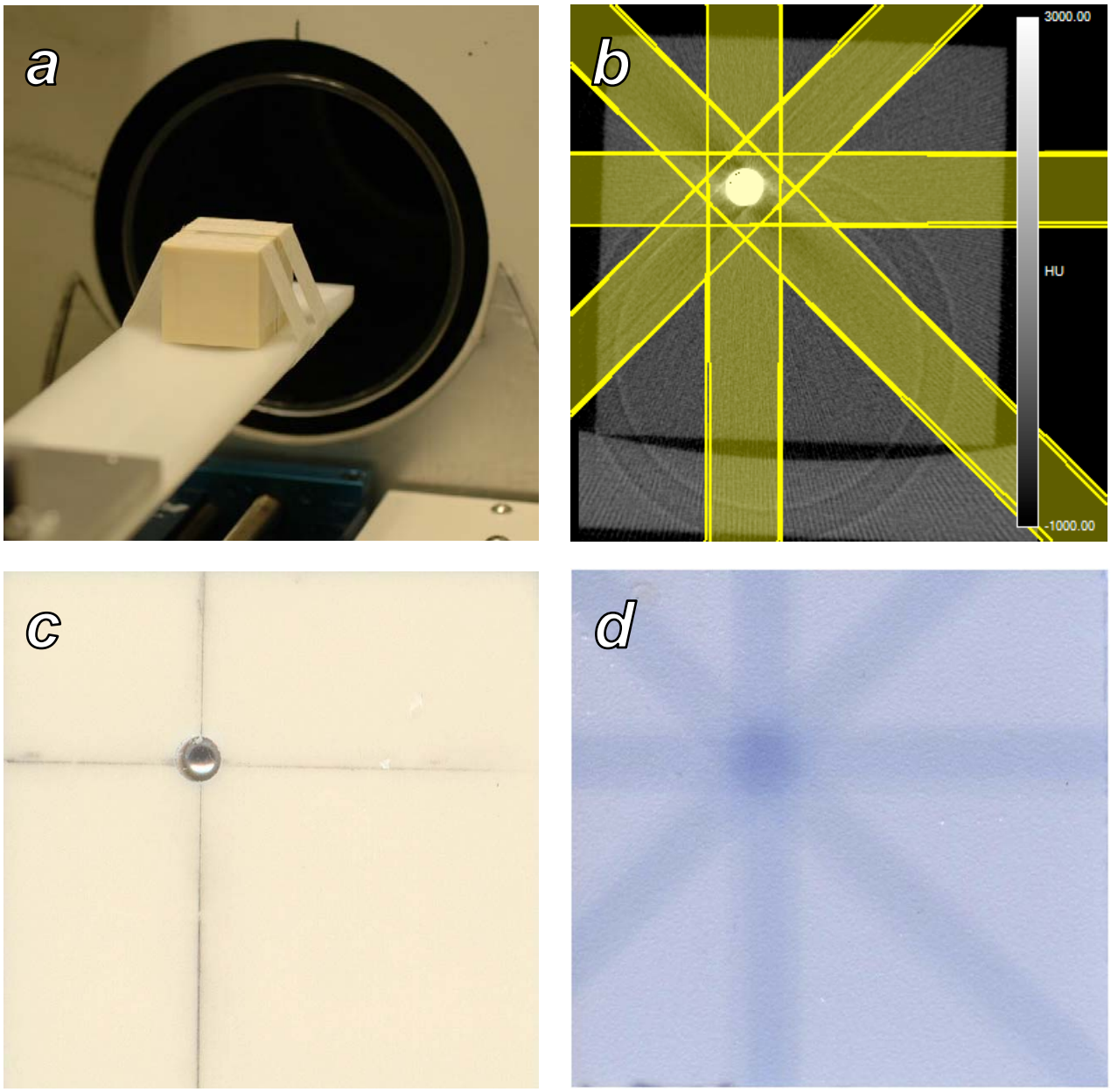

Figure 4

Click here to download Figure: hz_figures_ijrobp 4.pdf

Figure 4

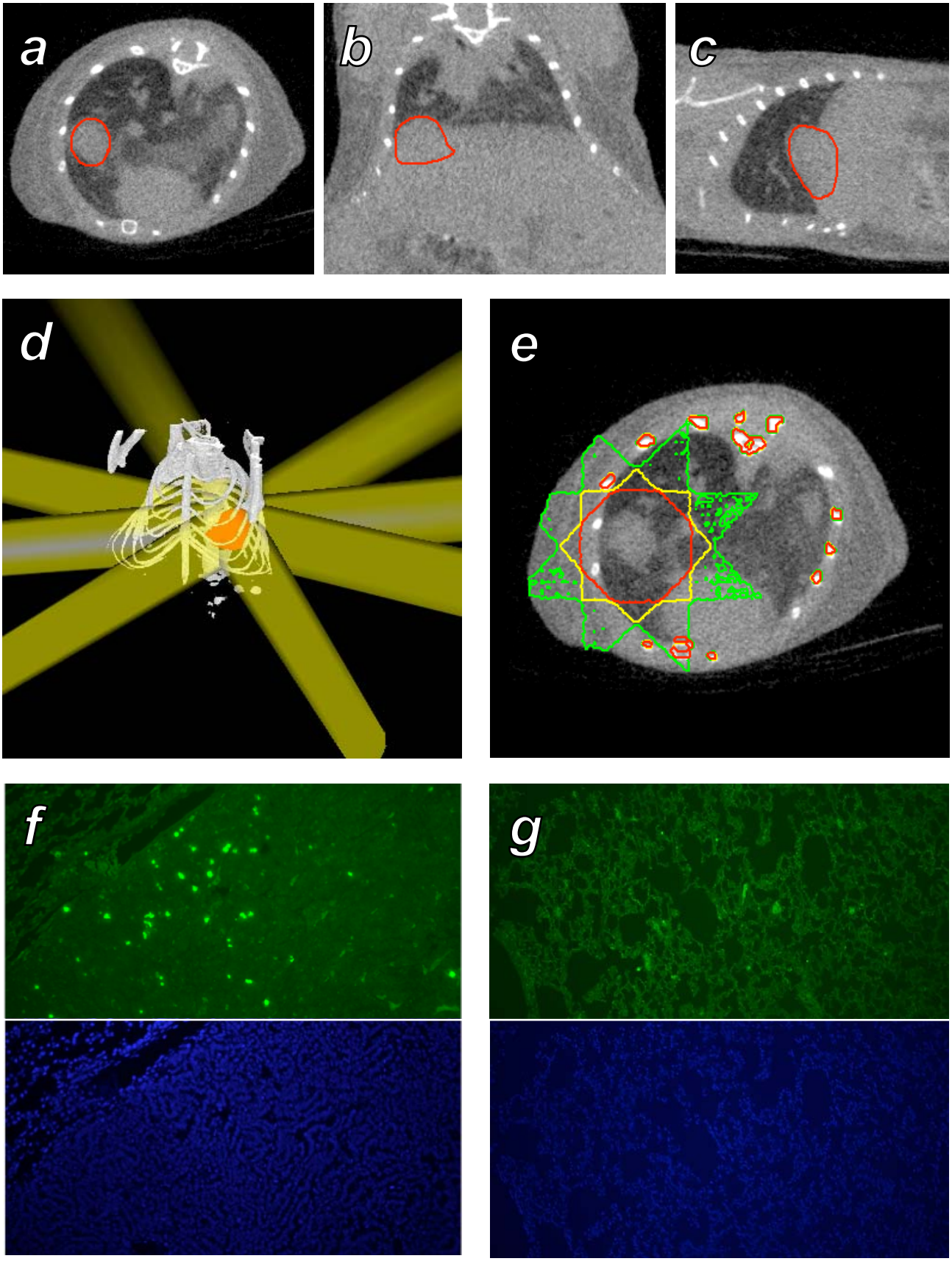

Table 1. Performance assessment of the collimator apparatus.

Isocenter aperture	Near Stage			Far Stage		
	Error	Closing time	Opening time	Error	Closing time	Opening time
16 mm	0.16%	19 sec	23 sec	0.01%	16 sec	16 sec
10 mm	0.25%	19 sec	24 sec	0.07%	19 sec	19 sec
5 mm	0.19%	24 sec	24 sec	0.24%	19 sec	19 sec
2 mm	0.79%	42 sec	26 sec	0.32%	24 sec	20 sec